The American Journal of Pathology, Vol. 182, No. 3, March 2013

ELSEVIER

The American Journal of
PATHOLOGY
ajp.amjpathol.org

GASTROINTESTINAL, HEPATOBILIARY, AND PANCREATIC PATHOLOGY

Intestinal Epithelial Cell—Derived μ-Opioid Signaling Protects against Ischemia Reperfusion Injury through PI3K Signaling

Jason R. Goldsmith,* Ernesto Perez-Chanona,* Prem N. Yadav,* Jennifer Whistler,† Bryan Roth,* and Christian Jobin*‡

From the Department of Pharmacology, University of North Carolina School of Medicine, Chapel Hill, North Carolina; the Neurosciences Graduate Program,† University of California, San Francisco, California; and the Department of Microbiology and Immunology,‡ University of North Carolina, Chapel Hill, North Carolina*

Accepted for publication November 12, 2012.

Address correspondence to Christian Jobin, Ph.D., Department of Medicine, Pharmacology, Immunology/Microbiology, University of North Carolina, Chapel Hill, NC 27599. E-mail: job@med.unc.edu.

Intestinal ischemia has a wide variety of causes, including, but not limited to, atherosclerosis, thrombosis, hypotension, and chronic inflammation. In severe cases, ischemic injury can result in death. μ-Opioid receptor (MOR) signaling has previously been shown to protect against chemically induced colitis, but the cellular origin of this effect remains unknown. Herein, we evaluated the role of intestinal epithelial cell (IEC)—derived MOR signaling in host responses to ischemia/reperfusion-induced injury. Ileal ischemia was accomplished through obstruction of the distal branches of the superior mesenteric artery (60 minutes) and reperfusion for 90 minutes (ischemia-reperfusion). Floxed-MOR mice were crossed to Villin-cre transgenic mice to selectively delete the *MOR* gene in IECs ($MOR^{IEC-/-}$). Radio-ligand binding assays demonstrated selective loss of MOR signaling in IECs of $MOR^{IEC-/-}$ mice. The s.c. administration of the MOR agonist, [D-Arg2, Lys4] dermorphin (1—4) amide (DALDA), 10 minutes before surgery protected against both ischemic and reperfusion phases of intestinal injury, an effect abolished in $MOR^{IEC-/-}$ mice. This cytoprotective effect was associated with enterocyte-mediated phosphoinositide 3-kinase (PI3K)/glycogen synthase kinase 3β signaling and decreased apoptosis, as determined by IHC and caspase-3 processing. PI3K blockade with Ly294002 resulted in loss of MOR-mediated cytoprotective function. Together, these data show that IEC-derived μ-opioid signaling uses the PI3K pathway to protect cells against the damaging effect of ischemia-reperfusion. Targeting MOR signaling may represent a novel mean to alleviate intestinal injury and promote the wound-healing response. *(Am J Pathol 2013, 182: 776—785; http://dx.doi.org/10.1016/j.ajpath.2012.11.021)*

The gastrointestinal epithelium performs a wide array of functions for the host, including secretion/absorption of nutrients, innate immune surveillance, and a physical barrier against the rich, diverse, and potentially immunogenic luminal contents. Therefore, preserving the integrity and maintaining intestinal barrier function are critical for host homeostasis. At the forefront of the intestinal barrier lies a single monolayer of intestinal epithelial cells (IECs),[1] which form a tight network of cells through the formation of tight junctions between IECs. These tight junctions are a critical component of the epithelium, and are necessary for the maintenance of the barrier during epithelial injury.[2,3] The epithelium is a dynamic system with highly migratory and proliferative IECs that help maintain and replace the barrier.[3] These active cells require constant high levels of blood flow to maintain their function. The superior mesenteric artery supplies blood to the small intestine and proximal two thirds of the large bowel, whereas the inferior mesenteric artery supplies the last third of the colon.[4—6] These arteries are supplemented by significant collateral blood flow to ensure proper intestinal function.[4—6]

Various events, such as chronic inflammation,[7] infection,[1] medications,[8,9] and ischemia, can all result in the loss

Supported by NIH grants R01DK047700 (C.J.), R01DK073338 (C.J.), and F30DK085906 (J.R.G.) and an NIH contract 271200800025C-6-0-1 (B.R.).

J.R.G. and E.P.-C. contributed equally to this work.

http://dx.doi.org/10.1016/j.ajpath.2012.11.021

of the intestinal barrier,[4,10] with deleterious consequences for the host. Among these various conditions, intestinal ischemia has been associated with severe disruption of small intestinal barrier function and integrity. Intestinal ischemia results in tissue hypoxia, which can cause induction of cellular apoptosis and loss of the protective epithelial layer. In addition to ischemia, the intestine can experience various levels of hypoxia because of atherosclerotic blockade, hemorrhage, venous emboli, surgical clamping, and cardiac tamponade.[10] In all of these cases, enteric blood supply must be reduced by at least 50% to overcome compensatory mechanisms.[4] Paradoxically, the restoration of blood flood (reperfusion) enhances the damage to the intestine through the introduction of oxygen free radicals and increased immune cell activation.[10] In severe cases, ischemia/reperfusion (I/R) injury can result in multiple organ dysfunction syndrome, with a mortality rate of approximately 30%.[11]

I/R-induced injury occurs in a multistep manner. In the first phase, the impaired blood flow to the epithelium generates an adaptive response involving the activation of protective signaling events that induce activity of different transcription factors, such as hypoxia-inducible factor[12] and NF-κB.[13] In the second phase, the adaptive response is generally overwhelmed by the rapid re-introduction of blood flow/oxygen (reperfusion), which enhances and sustains the inflammatory response.[10] Finally, the sustained intestinal immune response compromises the intestinal barrier function of the epithelium, allowing bacterial translocation across the mucosa, leading to bacteremia and sepsis, and generating a positive feedback loop of inflammation and intestinal damage.[10]

Unfortunately, current treatment of I/R injury is completely supportive, and no treatments focus on restoring the epithelial barrier defects that can lead to multiple organ dysfunction syndrome. Recently, we found that MOR signaling is protective against chemical-induced acute intestinal injury.[14] Rodent studies have demonstrated that opioids, such as morphine, are cardioprotective during ischemic episodes,[15,16] and these observations have been successfully extended to a randomized, double-blind, clinical trial.[17] MOR is a G protein–coupled receptor, and the cardioprotective effects of MOR signaling are believed to act through the $G_{\beta\gamma}$ subunit of the G_i protein coupled to MOR. Specifically, the $G_{\beta\gamma}$ subunit activates phosphoinositide 3-kinase (PI3K),[18] which can result in numerous prosurvival downstream signaling events, predominately mediated through Akt activation.[19] However, the role and cellular source of MOR signaling during I/R-mediated intestinal injury remain to be defined.

In these studies, we establish that MOR signaling is protective against both the ischemic and reperfusion phases of intestinal I/R-induced injury. Genetic approaches show that IEC-specific MOR signaling is the source of the cytoprotective responses. The MOR-mediated protective effect was, in part, attributed to PI3K signaling because pharmacological inhibition of the pathway abrogated the DALDA-induced beneficial impact.

Materials and Methods

Generation of $MOR^{IEC-/-}$ Mice

All mice were on the C57BL/6 background. Villin-Cre mice were crossed to $MOR^{f/f}$ mice, which contain loxP sites in introns 1 and 3, to generate mice lacking exons 2 and 3 of the MOR (Figure 1A). $MOR^{f/f}$ mice were generated by Xenogen Biosciences (Hopkinton, MA) using homologous recombination. Tail snips were collected from all pups generated from crosses, and genomic DNA was isolated using a Qiagen Blood and Tissue Kit (Qiagen, Valencia, CA). Mice were bred to generate the homozygote $MOR^{f/f}$ allele and the *Villin-Cre* gene. Primers used for genotyping were as follows: *Villin-Cre* promoter (5′-TAAGAAAGGATCATCATCAAAGCCGG-3′ and 5′-GTGAAACAGCATTGCTGTCACTT-3′) and Flox-*Oprm1* (5′-GTGTTTAAACATAGGTACAAGATATTCCCAAGCGAGA-3′ and 5′-GTCTCGAGCTGAGATTTAGGAAAGGTGTCGAATTATTG-3′).

For phenotypic analysis, RNA was isolated from enterocytes and splenocytes as previously described,[20] and expression of *MOR*, *Oprm1*, and *Gapdh* was determined by RT-PCR. Amplicons were resolved on a 2% agarose gel and visualized using a Kodak Gel Logic Imager 200 series (Kodak, Rochester, NY). Primers used were as follows: *Oprm1* (amplicon, 569 bp; 5′-ACCTGGCTCCTGGCTCAACT-3′ and 5′- TGGACCCCTGCCTGTATTTTG-3′), *Villin1* (amplicon, 330 bp; 5′-CCCCCATCTTCCA-3′ and 5′-TGCCCTGCCAGATATATAACA-3′), CD45 (*Ptprc*) (amplicon, 70 bp; 5′-ATGGTCCTCTGAATAAAGCCCA-3′ and 5′-TCAGCACTATTGGTAGGCTCC-3′), *Gapdh* (amplicon, 240 bp; 5′-GGTGAAGGTCGGAGTCAACGGA-3′ and 5′-GAGGGATCTCGCTCCTGGAAGA-3′).[21]

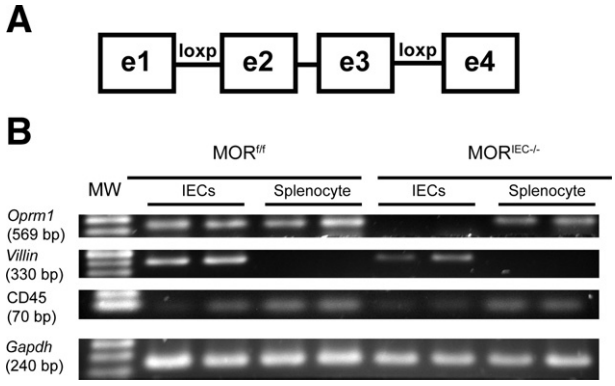

Figure 1 Generation of IEC-specific, *MOR* gene–deleted mice. **A:** Schematic representation of the exon-flanked *loxP* sites of $MOR^{f/f}$ mice. **B:** Real-time PCR analysis of MOR (oprm1) mRNA accumulation from IECs and splenocytes obtained from $MOR^{f/f}$ and $MOR^{IEC-/-}$ mice. *Villin* and CD45 are used as marker of enterocytes and immune cells, respectively. *Gapdh* is used as a loading control. Biological duplicates are shown.

I/R-Induced Injury

$MOR^{f/f}$ and $MOR^{IEC-/-}$ mice (C57BL/6 background) were maintained in standard housing cages in specific pathogen-free conditions. Mice ($n = 4$ to 6) were anesthetized under 1% isoflurane, supplemented by 10 mg/kg ketamine injected s.c. Vehicle (saline) or the MOR agonist, DALDA[22] (100% saline, 50 μg/kg) (US Biological, Swampscott, MA), was injected s.c. 10 minutes before surgery. The PI3K inhibitor, Ly294002 (0.25 mg/kg) (Calbiochem, Darmstadt, Germany), was injected i.p. 10 minutes before the administration of DALDA. A midline laparotomy was made, and peripheral branches of superior mesenteric artery were occluded with aneurysm clips (Kent Scientific, Torrington, CT), to generate a 2- to 3-cm region of ischemic ileum adjacent to the cecum. Collateral blood flow through the intestine was blocked using aneurysm clips across the intestine and collateral vessels, demarking the region of ischemic intestine. Hematoxylin was administered to the edges of ischemic tissue to mark them, and then the incision was closed with surgical staples. Ischemia was maintained for 60 minutes, and then the incision was re-opened, the clamps were removed, and the incision was reclosed. The mice were maintained in a heated room for a variable amount of time (0, 1.5, or 4 hours) without anesthesia for the reperfusion phase of injury. All animal experiments were approved by the Institutional Animal Care and Use Committee of the University of North Carolina, Chapel Hill (Chapel Hill, NC).

Murine Sample Collection and Histological Evaluation

Mice were anesthetized using isoflurane, and then sacrificed by cervical dislocation. The colon was dissected and flushed with ice-cold PBS, longitudinally splayed, Swiss rolled, fixed in 10% formalin for 24 hours, and then embedded in paraffin. Damage severity was evaluated using H&E-stained sections by blinded investigators (J.R.G., E.P.C.). The scoring system is based on an IEC apoptosis/necrosis system,[23] where a score of 1 signified a loss of only the villus tips; 2, loss of 50% of the villus; 3, a loss of the entire villus, but with maintenance of the crypt; and 4, complete loss of the epithelial layer. Fractional (to the nearest 0.5) scores were given, and the score was based on the average damage of the entire tissue section.

Cell Membrane Fraction Isolations

Primary IECs were isolated as previously described.[24] Briefly, small intestines and colons were opened longitudinally and washed, and IECs were separated from the underlining tissue by shaking the intestines in a solution containing 1.5 mmol/L EDTA (with 0.5 mmol/L dithiothreitol for colon sections) and proteinase inhibitors (Complete Mini; Roche Diagnostics GmbH, Penzberg, Germany) for 30 minutes at 37°C. The remaining tissue was filtered with a 0.45-μm cell culture filter to remove the underlying stroma, and samples from three mice were pooled and spun at 1000 × g for 5 minutes. Cells were lysed in chilled, hypotonic 50 mmol/L Tris-HCl, pH 7.4, solution for 30 minutes. Cell membrane isolates were then prepared by washing the lysate three times in standard binding buffer [50 mmol/L Tris-HCl, 10 mmol/L $MgCl_2$, and 0.1 mmol/L EDTA (pH 7.4)], followed by centrifugation at 21,000 × g. The lysate was then resuspended in the binding buffer and passaged through a 26-gauge needle to ensure homogenization, forming the final membrane suspensions used in the radioligand binding assays.

Brain membrane homogenates were made using cortex tissue. Brains were harvested from mice, and their cortices were dissected. The tissues were homogenized in standard binding buffer with proteinase inhibitors using a polytron (IKA Works Inc., Wilmington, NC), and then prepared in the same manner as the IECs in standard binding buffer. The protein concentration of each membrane suspension was determined by using a Bio-Rad quantification assay (Bio-Rad Laboratories, Hercules, CA).

Radioligand Binding Assay

Radioligand binding assays were performed by the Psychoactive Drug Screening Program at the University of North Carolina, Chapel Hill, using a modification of previously described procedures.[25] Membrane suspensions (50 μL) were incubated with 0.3, 0.6, 1.25, 2.5, 5, or 10 nmol/L H^3-[D-Ala2, N-MePhe4, Gly-ol]-enkephalin (DAMGO) (GE Healthcare, Piscataway, NJ), with or without 10 μmol/L naltrexone (Sigma-Aldrich, St. Louis, MO), for 1 hour at room temperature, shielded from light. Samples were then harvested by rapid filtration onto Whatman GF/B glass fiber filters presoaked with 0.3% polyethyleneimine using a 96-well Brandel harvester. Four rapid 500-μL washes were performed with chilled standard binding buffer to reduce nonspecific binding. The filter mats were dried, scintillant was melted onto the filters, and the radioactivity was counted using a Microbeta scintillation counter. Radioactivity of H^3-DAMGO was quantified by liquid scintillation counting, using EcoScint scintillation cocktail (National Diagnostics, Atlanta, GA). Raw data (decays per minute) were converted to fmols of ligand binding/mg of total tissue, using a detection efficiency of 0.5 to convert from decays per minute to counts per minute.

IHC and Immunofluorescence

Immunohistochemical (IHC) staining was performed according to the manufacturer's specifications, as previously described.[20] Primary antibodies and dilutions were as follows: glycogen synthase kinase 3β (p-GSK3β; Ser9), 1:400 (Cell Signaling Technology, Beverly, MA); and p-AKT (Ser473), 1:50 (Cell Signaling Technology). IHC for activated caspase-3, 1:400 (R&D Systems, Minneapolis, MN) was performed as previously described.[26] All sections were counterstained

Table 1 $MOR^{IEC-/-}$ Enterocytes Do Not Bind μ Ligand

	DAMGO B_{max}	
Mouse strain	Cortex, nmol/L	Enterocyte, nmol/L
$MOR^{f/f}$	165.6 ± 16.10	11.55 ± 4.397
$MOR^{IEC-/-}$	108.5 ± 13.10	No binding detected

Data are given as fmol/mg. Radioligand binding assays using the MOR-specific agonist H^3-DAMGO demonstrated an absence of intestinal binding in $MOR^{IEC-/-}$ mice. No statistically significant difference between $MOR^{f/f}$ and $MOR^{IEC-/-}$ binding was observed ($P = 0.0705$) in the cortex (brain) samples used as a positive control. $N = 4$ or 6 per group.

with hematoxylin. Only crypts that had two or more positively staining cells per 10 total crypts in a field of view were counted for IHC analysis.

A fluorometric TUNEL assay was performed using a DeadEnd Kit (Promega, Madison, WI), according to the manufacturer's protocols. Images were acquired using a Zeiss 710 microscope with a 20×, 1.4 numerical aperture objective (Carl Zeiss, Thornwood, NY). Zeiss Zen 2009 software (Carl Zeiss) was used for image acquisition. All images were acquired at room temperature.

RNA Isolation and Real-Time PCR

RNA isolation from ileal tissues and subsequent cDNA amplification and analysis were performed as previously described,[20] using an ABI Prism HT7700 (Applied Biosystems, Foster City, CA). The specificity and linearity of amplification for each primer set were determined by melting curve analysis and calculation of the slope from serial diluted samples. Relative fold changes were determined using the $\Delta\Delta C_T$ calculation method. Values were normalized to the internal control, glyceraldehyde-3-phosphate dehydrogenase (GAPDH) or β-actin. Primers were as follows: *Il6* (5′-CGGAGGCTTAATTACACATGTT-3′ and 5′-CTGGCTTTGTCTTTCTTGTTATC-3′),[21] *Il1b* (5′-GCCCATCCTCTGTGACTCAT-3′ and 5′-AGGCCACAGGTATTTTGTCG-3′),[14] *Gapdh* (5′-GGTGAAGGTCGGAGTCAACGGA-3′ and 5′-GAGGGATCTCGCTCCTGGAAGA-3′),[21] and β-*actin* (5′-TTACCAACTGGGACGACATG-3′ and 5′CTGGGGTGTTGAAGGTCTC-3′).

Bacterial Ribosomal 16S DNA

For all bacterial translocation assays, mice were subjected to 60 minutes of ischemia, followed by 4 hours of reperfusion, in the presence or absence of DALDA, as previously described. Mice were sacrificed, and their livers were harvested and weighed. To determine bacterial 16S ribosomal DNA (rDNA) loads, livers were incubated in lysis buffer [200 mmol/L NaCl, 100 mmol/L Tris-HCl (pH 8), 20 mmol/L EDTA, and 20 mg/mL lysozyme] for 30 minutes at 37°C, and then in 1% SDS and 0.35 mg/mL proteinase K (Sigma-Aldrich) for 30 minutes at 60°C. The homogenates were further lysed in a 60% volume of phenol/chloroform/isoamyl alcohol mixture (25:24:1) using a Mini Bead Beater 8 (Biospec, Bartleville, OK). DNA was isolated using a chloroform/isoamyl alcohol (24:1) solution and precipitated with 2.5× volumes of ethanol with 3 mol/L sodium acetate (pH 5.2) overnight at −20°C. The pellet was resuspended in Tris buffer (10 mmol/L, pH 8), and a Qiagen

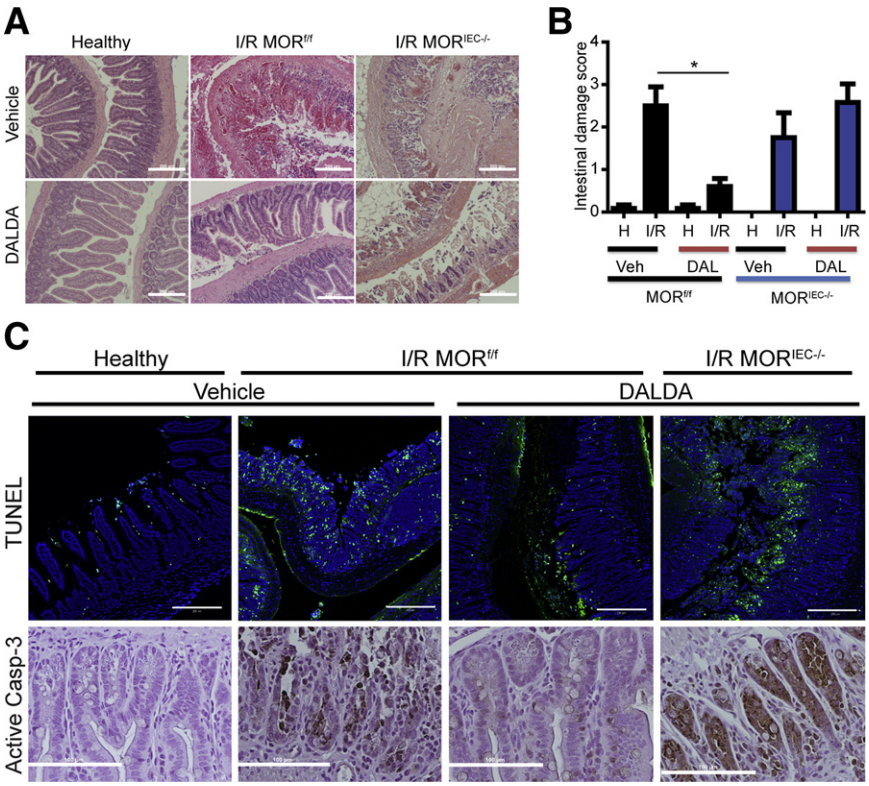

Figure 2 DALDA (DAL) administration protects against I/R-induced injury. DALDA, 50 μg/kg, was administered s.c. to $MOR^{f/f}$ and $MOR^{IEC-/-}$ mice 10 minutes before I/R exposure. Healthy tissues (H) represent a nonischemic region of the small bowel adjacent to the damaged area. **A**: Representative H&E images of ileal Swiss rolls. $N = 5$ to 6 per group. **B**: Histological damage scores show DALDA-mediated protection from I/R injury only in mice with functional IEC-derived MOR signaling ($MOR^{f/f}$). $N = 5$ to 6 per group. $^*P < 0.05$. **C**: The TUNEL assay demonstrates decreased apoptotic/necrotic IECs in DALDA-treated mice with functional IEC-derived MOR signaling. Cells with fragmented DNA are stained green, whereas DAPI counterstain marked all intestinal cells. Data are representative of three sections per group, from two different mice. IHC analysis of activated caspase-3 (Casp-3) from an ileal section of DALDA-treated $MOR^{f/f}$ and $MOR^{IEC-/-}$ mice showed decreased caspase-3 staining in mice with functional IEC-derived MOR signaling. Images are representative of two different mice. Scale bars: 200 μm (**A** and **B**); 100 μm (**C**). Veh, vehicle.

DNeasy Blood and Tissue Kit (Qiagen) was used according to the manufacturer's protocol. Isolated DNA was subjected to real-time PCR, as previously described, using the following primers: universal *16s rDNA* (5′-GTGSTGCAYGGYTGTC-GTCA-3′ and 5′-ACGTCRTCCMCACCTTCCTC-3′), normalized to murine *Gapdh* (as previously described).

CMT-93 Cell Culture and Stimulation

Murine rectal carcinoma cells (passage 33 to 59) (ATCC, Manassas, VA) were cultured in Dulbecco's modified Eagle's medium high glucose, as previously described.[27] Cells were starved overnight in Opti-MEM (Cellgro, Manassas, VA) and then treated with DALDA (10 μmol/L) for the times indicated. MOR signaling was inhibited with the opioid antagonist, naloxone (Sigma-Aldrich; 10 μmol/L in dimethylsulfoxide), 30 minutes before DALDA exposure. Protein synthesis was blocked with cycloheximide (Sigma-Aldrich) (50 μg/mL). Cells were directly lysed in one times Laemmli buffer, and protein concentration was measured using a Bio-Rad quantification assay.

Western Blot Analysis

Proteins (30 μg) were separated using 10% SDS-PAGE, transferred to nitrocellulose membranes, and then probed with antibodies specific to cleaved-caspase-3, *p*-GSK3β (Ser9), and *p*-AKT (Ser473), at a 1:1000 dilution, and GSK3β and AKT at a 1:2000 dilution (Cell Signaling Technology) in 5% nonfat milk, 2% bovine serum albumin in Tris-buffered saline—Tween (0.1%), and β-actin (1:10,000) (MP Biomedical, Solon, OH), followed by the appropriate horseradish peroxidase—conjugated secondary antibody (1:10,000) (GE Healthcare, Piscataway, NJ). The immune complexes were detected using chemiluminescence.

Apoptosis Assays

Murine rectal-carcinoma CMT-93 cells were plated to 70% confluence in 8-well chamber cells (Thermo Scientific, Waltham, MA), and exposed to 1 μmol/L staurosporine (Sigma-Aldrich) for 6 hours concurrently with 10 μmol/L DALDA and/or 1 μmol/L wortmannin. A fluorometric TUNEL assay was then performed as previously described, according to the manufacturer's protocol.

Statistical Analysis

Unless specifically noted, statistical analyses were performed using GraphPad Prism version 5.0a (GraphPad, La Jolla, CA). Comparisons of mouse studies were made with a nonparametric, one-way analysis of variance, and a Kruskal-Wallis test with Dunn's multiple comparison post test. Further comparisons made between mice were analyzed using a *U*-test at a 95% CI. *In vitro* migration data and cell counting were compared with Student *t*-tests, at a 95% CI. Radioligand binding assays were analyzed using a nonlinear fit (single-binding site) function, built into Prism. All graphs depict means ± SEM. Experiments were considered statistically significant if $P < 0.05$.

Results

Generation of IEC-Specific, *MOR* Gene—Deleted Mice

To define the role of IEC-derived MOR signaling in the intestine, we crossed floxed-MOR mice ($MOR^{f/f}$) to Villin-Cre mice to generate IEC-specific gene—deleted mice ($MOR^{IEC-/-}$) (Figure 1A). PCR analysis showed MOR (Oprm1) mRNA accumulation in purified IECs and splenocytes from $MOR^{f/f}$ mice, whereas the transcript was absent in the IECs of $MOR^{IEC-/-}$ mice (Figure 1B). MOR mRNA accumulation was detected in splenocytes isolated from $MOR^{IEC-/-}$ mice, showing the specificity of *MOR* gene deletion (Figure 1B). Radioligand binding assays revealed a lack of detectable binding of the MOR-specific ligand ^{3}H-DAMGO in IEC cells isolated from $MOR^{IEC-/-}$ mice compared with $MOR^{f/f}$ mice (Table 1). ^{3}H-DAMGO binding to brain (cortex) cell membrane extracts was not significantly altered in $MOR^{IEC-/-}$ mice. These findings confirmed that MOR signaling is functionally ablated in IECs in $MOR^{IEC-/-}$ mice.

IEC μ-Opioid Signaling Protects against I/R Injury

To address the cell type—specific role of MOR signaling in intestinal injury response, we subjected mice to an episode of I/R-induced injury, in which the peripheral branches of

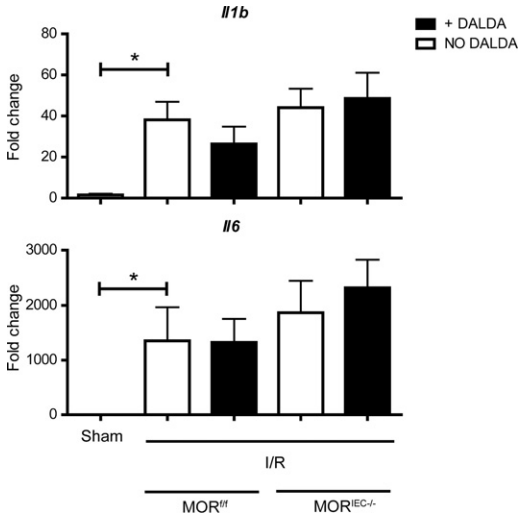

Figure 3 The MOR-mediated cytoprotective effect does not correlate with decreased cytokine production. Mice were treated with DALDA and exposed to I/R, as described in the legend to Figure 2. Il1b, Il6, and tumor necrosis factor (Tnf) mRNA ileal tissue levels were determined using an ABI Prism7900HT. Data were processed using the $\Delta\Delta C_T$ method, normalized to β-*actin*, and set relative to sham—operated on mouse tissue. No statistical significance was noted between any of the ischemic tissue groups. $P < 0.0317$ for *Il1b*, $P < 0.0159$ for *Il6* for the comparison between the sham and all ischemic groups. $N \geq 3$ per group. *$P < 0.05$.

the superior mesenteric artery were clamped for 60 minutes (ischemic phase), followed by 90 minutes of reperfusion. As shown in Figure 2, I/R-induced injury results in epithelium denudement, with partial to complete ablation of the crypts, alongside immune cell infiltration into the lamina propria. Interestingly, the administration of 50 μg/kg DALDA dramatically reduced I/R-mediated tissue damage compared with untreated mice, as shown by histological damage assessment (2.5 versus 0.6; $P < 0.05$) (Figure 2, A and B). However, DALDA was unable to protect $MOR^{IEC-/-}$ mice from I/R-induced injury compared with $MOR^{f/f}$ mice (1.75 versus 2.58; $P = 0.2920$) (Figure 2, A and B).

Because of hypoxic conditions, I/R-induced injury leads to increased IEC apoptosis with associated disruption of intestinal barrier function.[4,5,10] A fluorescent TUNEL assay showed enhancement of fragmented DNA, indicative of apoptosis/necrosis in injured mice, which was absent in mice treated with DALDA (Figure 2C). DALDA-mediated reduction of DNA fragmentation was ablated in $MOR^{IEC-/-}$ mice (Figure 2C). To specifically address the role of apoptosis in DALDA-mediated protection, we investigated the level of caspase-3 activation using IHC. Interestingly, caspase-3 activation was strongly reduced after DALDA treatment, an effect abrogated in $MOR^{IEC-/-}$ mice (Figure 2C). These findings indicate that IEC-derived MOR signaling is critical for the DALDA-mediated protective effect on the epithelium.

Interestingly, I/R-induced *Il1b* and *Il6* mRNA accumulation was not modulated by DALDA administration, nor was it affected by the status of MOR expression (Figure 3). A similar, but less robust, pattern of induction was noticed with tumor necrosis factor mRNA (data not shown).

Because I/R-induced injury is a multiphase process, we next investigated the role of MOR signaling during the early ischemic phase of intestinal injury. Administration of DALDA

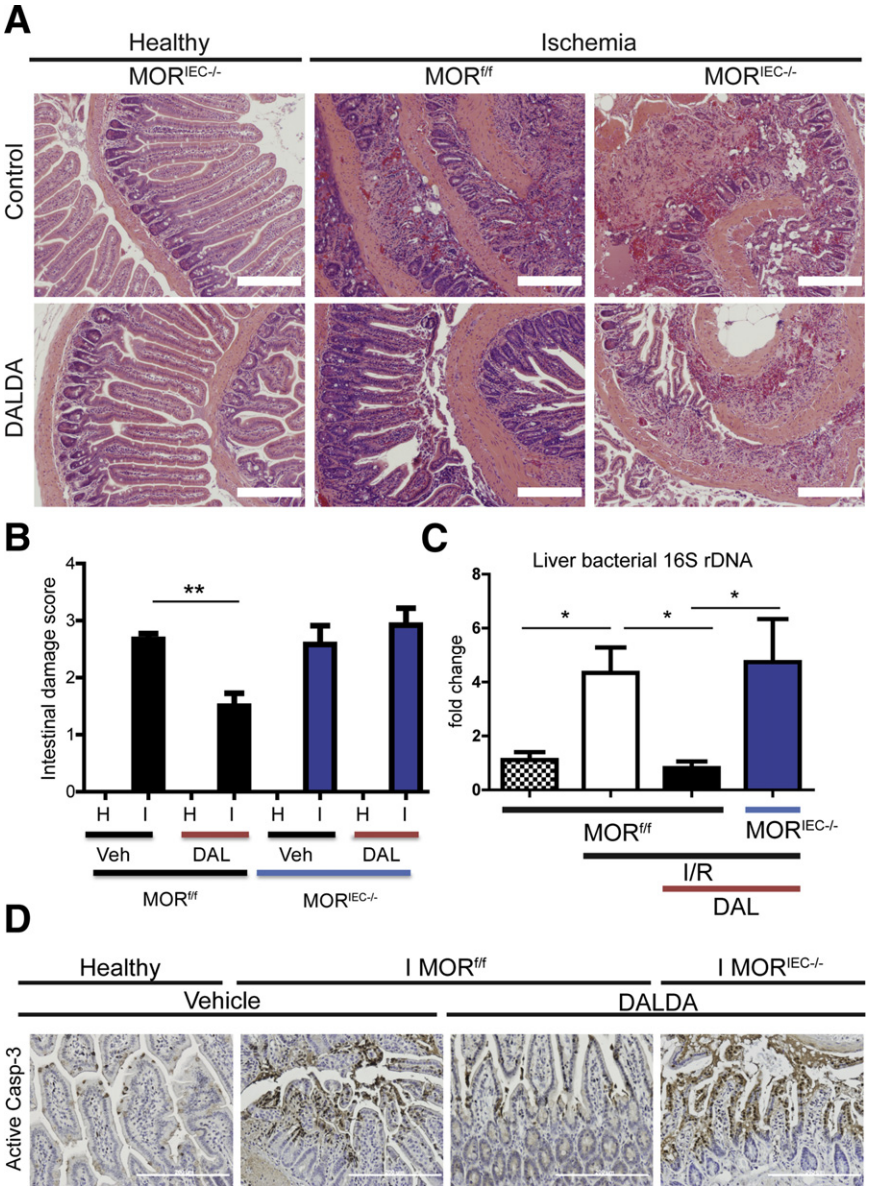

Figure 4 DALDA (DAL) administration protects against ischemia-induced injury and attenuates bacterial translocation. DALDA, 50 μg/kg, was administered s.c. to $MOR^{f/f}$ and $MOR^{IEC-/-}$ mice 10 minutes before ischemia (I) exposure (60 minutes). Healthy tissues (H) represent a nonischemic region of the small bowel adjacent to the damaged area. **A:** Representative H&E images of ileal Swiss rolls. **B:** Histological damage scores show DALDA-mediated protection from ischemia injury only in mice with functional IEC-derived MOR signaling ($MOR^{f/f}$). $N = 5$ to 6 per group. **C:** PCR quantification of total bacterial 16S DNA at 4 hours of reperfusion shows that MOR-mediated protection results in decreased bacterial dissemination to the liver. Data were analyzed by the $\Delta\Delta C_T$ method, normalized to murine Gapdh, and compared with control. $N = 4$ per group. **D:** IHC analysis of activated caspase-3 from an ileal section of DALDA-treated $MOR^{f/f}$ and $MOR^{IEC-/-}$ mice shows that enterocyte MOR signaling confirms protection from apoptosis during the ischemic phase of injury. Images are representative of three different mice. Scale bars: 200 μm (**A** and **D**). Veh, vehicle. $^*P < 0.05$, $^{**}P < 0.01$.

protected against the induction of intestinal damage during the ischemic phase (2.7 versus 1.5; $P < 0.01$), an effect dependent on the presence of functional IEC-MOR signaling (Figure 4, A and B). These data suggest that IEC-derived MOR signaling protects against the deleterious effect of ischemia.

One potentially serious outcome of intestinal ischemia is multiorgan dysfunction syndrome,[11] which results from bacterial translocation and dissemination after loss of the intestinal barrier function.[13] To assess for the presence of extra-intestinal bacteria during I/R-induced injury, we measured the bacterial 16S rDNA in the liver. Increased bacterial 16S rDNA (approximately fourfold) in the liver of I/R-exposed $MOR^{f/f}$ mice was significantly decreased in DALDA-treated mice, whereas this beneficial effect was lost in $MOR^{IEC-/-}$ mice (Figure 4C). These findings indicate that DALDA prevented the initial ischemia-induced insult and halted bacterial translocation to extra-intestinal organs.

TUNEL (data not shown) and IHC analyses of activated caspase-3 demonstrated that IEC-MOR signaling conferred protection during the ischemic phase of injury through up-regulation of prosurvival/anti-apoptotic signals (Figure 4D).

MOR-Mediated Protection Involves PI3K-Mediated GSK3β Phosphorylation

We previously showed *in vitro* that IEC wound-healing responses are dependent on PI3K/GSK3β signaling.[28] To test the role of the PI3K/GSK3β pathway in the MOR-mediated protective effect, we stimulated CMT-93 cells with 10 μmol/L DALDA for a variable period and performed Western blot analysis. DALDA rapidly increased both Akt and GSK3β phosphorylation in CMT-93 cells (Figure 5A). Interestingly, the protein synthesis inhibitor, cycloheximide, failed to block DALDA-induced GSK3β phosphorylation, indicating a direct effect on the PI3K/Akt/GSK3β pathway (Figure 5B). To better define the role of MOR in DALDA-mediated GSK3β phosphorylation, we treated CMT-93 cells with 10 mmol/L of the opioid antagonist, naloxone.[22] DALDA-induced GSK3β phosphorylation was blocked in naloxone-exposed cells compared with control, highlighting the key role of MOR in this process (Figure 5C). Altogether, these findings suggest that DALDA signals through MOR to activate the PI3K/GSK3β pathway without the need of *de novo* protein synthesis.

Because cellular apoptosis is a key event in I/R-induced intestinal injury, we determined the impact of DALDA and PI3K/GSK3β signaling on staurosporine-induced CMT-93 cell apoptosis. The TUNEL assay shows that DALDA mediated blockade of staurosporine-induced apoptosis in CMT-93 cells is attenuated following exposure to 1 μmol/L wortmannin (Figure 6A). Similarly, DALDA-mediated blockade of caspase-3 processing was reversed in wortmannin-treated CMT-93 cells (Figure 6B). Together, these findings indicate that PI3K activation is necessary for a DALDA-mediated anti-apoptotic effect.

To expand these observations *in vivo*, we performed IHC analysis on DALDA-treated mice. Interestingly, IEC-specific

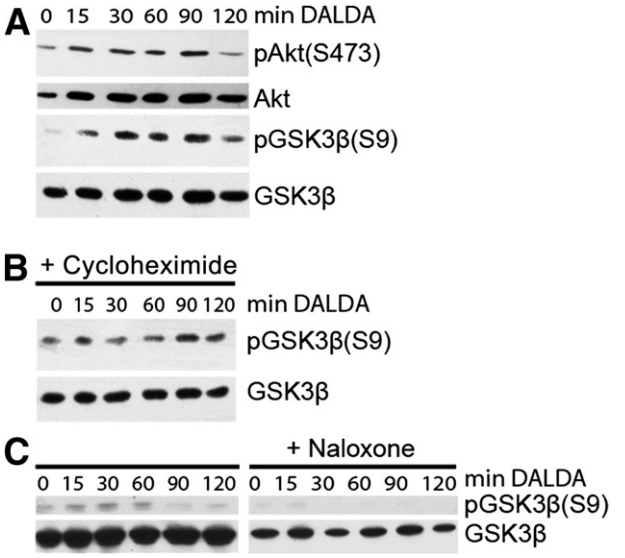

Figure 5 MOR signaling directly induces GSKβ phosphorylation in a PI3K-dependent manner in CMT-93 cells. CMT-93 cells were stimulated with 10 μmol/L DALDA for the indicated time in the presence or absence of 50 μg/mL cycloheximide or 10 mmol/L MOR inhibitor, naloxone. Proteins were extracted and subjected to Western blot analysis. **A**: Kinetic analysis of Akt and GSK3β phosphorylation. **B**: DALDA-mediated GSK3β phosphorylation is unaffected in cycloheximide-treated cells. Data are representative of three independent experiments. **C**: DALDA-mediated GSK3β phosphorylation is abrogated in naloxone-treated cells. Data are representative of three independent experiments.

Akt and GSK3β phosphorylation is enhanced in DALDA-treated $MOR^{f/f}$ mice compared with the vehicle-treated mice (Figure 7, A and B). We further quantified *p*-GSK3β staining and found increased staining in the crypts of DALDA-treated $MOR^{f/f}$ mice compared with the vehicle-treated mice (7.2 versus 3.9; $P < 0.01$) (Figure 7C). Finally, we observed that activation of these signaling pathways was abrogated in DALDA-treated $MOR^{IEC-/-}$ mice (Figure 7, A–C), demonstrating that these effects were a result of direct enterocyte-mediated MOR signaling.

To determine the functional role of PI3K signaling in the DALDA-mediated protective effect, $MOR^{f/f}$ mice were treated with 0.25 mg/kg, i.p., of the PI3K inhibitor, Ly294002. Interestingly, the DALDA-mediated protective effect against I/R-induced injury was lost in mice treated with Ly294002 (Figure 8, A and B). In addition, the administration of Ly294002 resulted in decreased DALDA-mediated induction of GSK3β phosphorylation and reduction in baseline GSK3β phosphorylation levels (Figure 8, C and D). Furthermore, DALDA-mediated blockade of caspase-3 processing in injured tissue was reversed after exposure to Ly294002, indicating the key role of IEC-derived PI3K signaling in the cytoprotective effects of DALDA (Figure 8E).

Discussion

Intestinal ischemia/reperfusion injury is a serious pathological condition with a potentially lethal sequel, including multiple

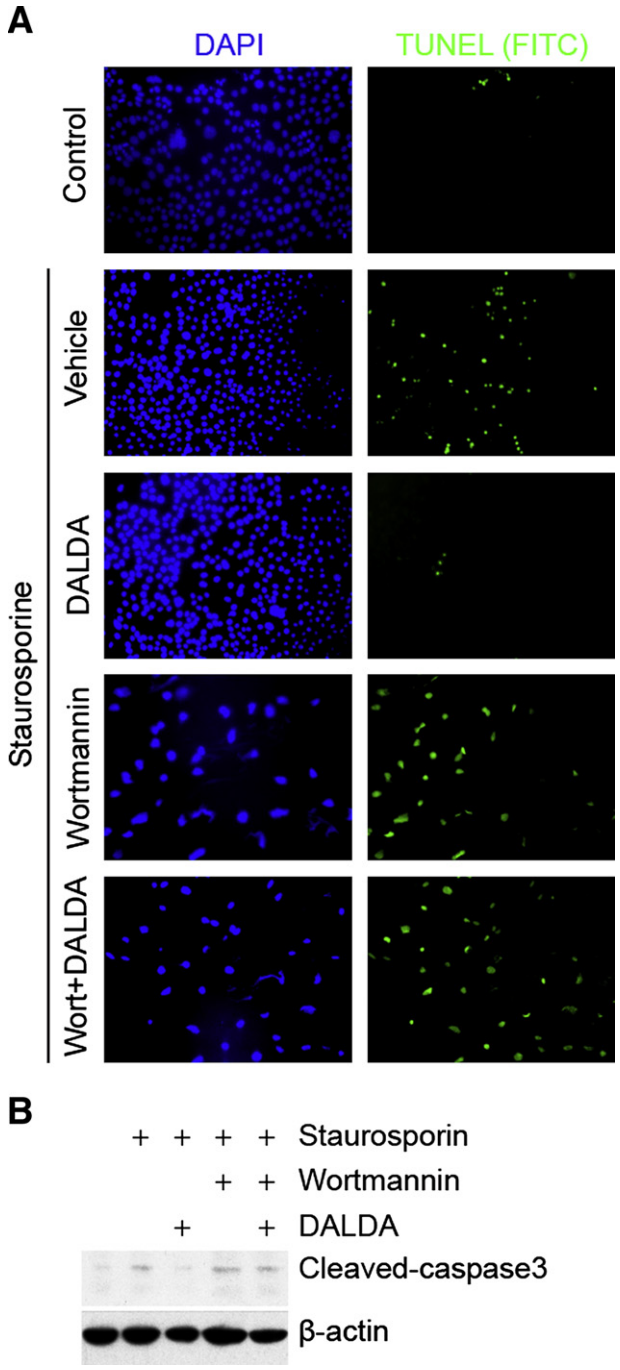

Figure 6 DALDA-induced protection from apoptosis is PI3K dependent. CMT-93 cells were exposed to 1 μmol/L staurosporine for 6 hours in the presence or absence of 10 μmol/L DALDA and/or 1 μmol/L wortmannin (Wort). **A**: Apoptosis was detected by TUNEL staining. Cells were also stained with DAPI as a control. Representative images of three independent experiments are shown. **B**: DALDA prevents staurosporine-induced caspase-3 processing in CMT-93 cells. Cells were treated as previously described, and proteins were extracted and subjected to caspase-3 Western blot analysis. Actin was used as a loading control. Representative data of three independent experiments are shown. FITC, fluorescein isothiocyanate.

organ dysfunction syndrome.[11] Unfortunately, no therapeutic strategies are available to treat the underlying intestinal injury that drives many of these sequels. Although opioid agonists have been shown to protect various organs against injury, including the intestine and heart, the cellular compartment(s) mediating these effects have remained elusive. Because IEC responses to various injuries, including inflammation, radiation, and I/R, are critical for the maintenance of intestinal barrier function,[13,29–31] we speculated that these cells drive the DALDA-mediated protective effect. Indeed, selective genetic removal of MOR signaling in IECs abrogated the cytoprotective action of DALDA after I/R exposure. Because the extent of intestinal injury after I/R-induced injury is similar between $MOR^{f/f}$ and $MOR^{IEC-/-}$ mice, we conclude that MOR signaling is protective only in the presence of an exogenous ligand (eg, DALDA). In addition, adjacent healthy tissue showed no alterations in villus length or crypt numbers in $MOR^{IEC-/-}$ mice. Furthermore, the administration of DALDA did not result in increased villus length or crypt numbers in the healthy tissue of $MOR^{f/f}$ mice. These findings suggest that DALDA/MOR-mediated protection is a direct result of tightly regulated MOR signaling that occurs only in injured tissue.

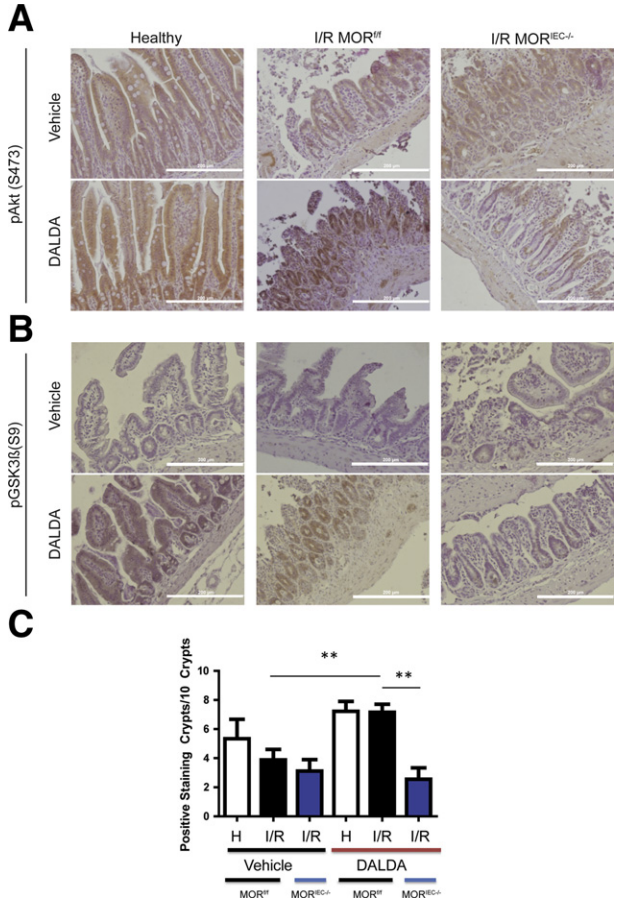

Figure 7 DALDA-induced protection from I/R injury correlates with enterocyte AKT and GSK3β phosphorylation. Mice were treated with DALDA and exposed to I/R, as described in the legend to Figure 2. Healthy tissues (H) represent a nonischemic region of the small bowel adjacent to the damaged area. **A**: Representative IHC of ileal Swiss rolls stained for *p*-Akt. $N = 2$ per group. **B**: Representative IHC of ileal Swiss rolls stained for *p-GSK3β*. $N = 3$ per group. **C**: Number of *p*-GSK3β—positive crypts per 10 crypts. $N = 3$ mice per group, with three random fields of view per mouse. Analysis was performed by one-way analysis of variance with Tukey's post test. $^{**}P < 0.01$. Scale bars: 200 μm (**A** and **B**).

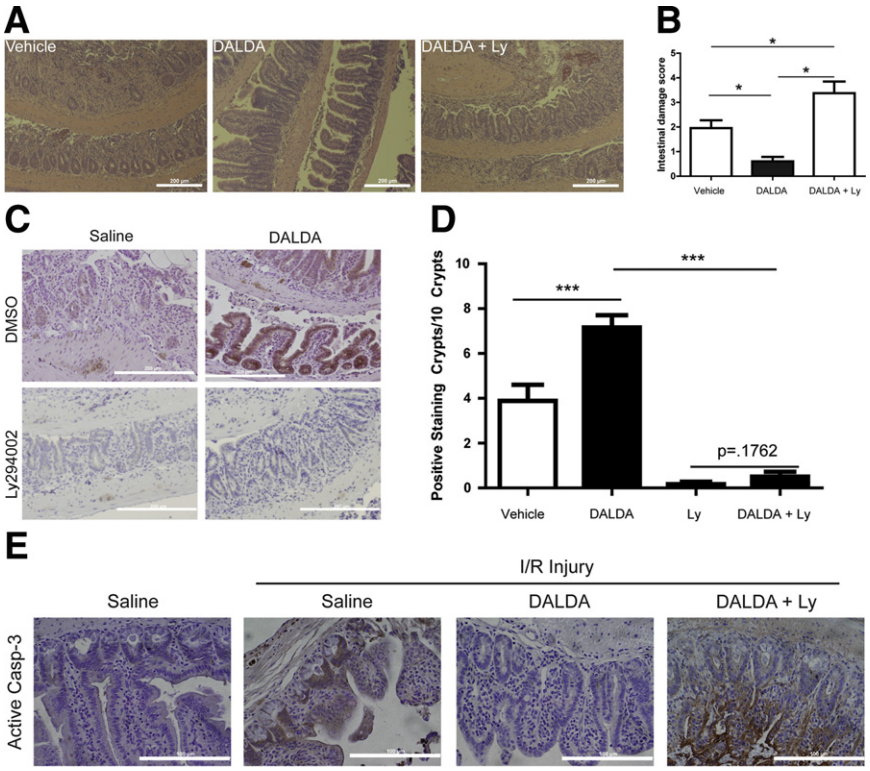

Figure 8 DALDA-mediated cytoprotection is PI3K dependent. The PI3K inhibitor, Ly294002 (Ly), was administered to $MOR^{f/f}$ and $MOR^{IEC-/-}$ mice at 0.25 mg/kg, i.p., 10 minutes before injection of vehicle or DALDA and then exposed to I/R, as described in the legend to Figure 2. Histological characteristics (**A**) and histological damage scores (**B**) show that DALDA-mediated protection from I/R injury requires functional PI3K signaling. $N = 4$ to 11 per group. **C** and **D**: DALDA-induced *p*-GSK3β phosphorylation is ablated in mice treated with Ly294002. Scale bar = 200 μm. Positive staining *p*-GSK3β crypts per 10 total crypts. Results are from five to six mice per group, with two random fields of view per mouse. Analysis was performed by one-way analysis of variance with Tukey's post test. **E**: IHC for activated caspase-3 (Casp-3) shows that DALDA-mediated apoptosis prevention is PI3K dependent. Representative images from four mice per group are shown. Scale bars: 200 μm (**A** and **C**); 100 μm (**E**). $^*P < 0.05$, $^{***}P < 0.001$. DMSO, dimethylsulfoxide.

Interestingly, DALDA administration had no significant modulatory effect on I/R-induced Il6, Il1b, and tumor necrosis factor mRNA expression levels. Because $MOR^{IEC-/-}$ mice have functional MOR in the immune compartment, these findings suggest that DALDA/MOR primary therapeutic effects are not immune cell mediated. Also, this suggests that the induction of inflammatory cytokines in the intestine in the early stages of I/R-induced injury is driven by the presence of hypoxic conditions more than the extent of injury to the tissue itself. This is compatible with the reported effect of hypoxia on inflammatory gene expression observed in the intestine and may represent an adaptive response to promote resistance to apoptosis in IECs.[32,33]

We observed the protective effect of DALDA in the ischemic phase of injury, during which IECs typically undergo apoptosis because of prolonged hypoxia,[4,5,10] suggesting that anti-apoptosis may be the primary mechanism of protection conferred by DALDA. Previous reports showed that MOR activates the proproliferative and survival signaling pathway PI3K/Akt/GSK3β in numerous *in vitro* systems[18] and during cardiac ischemia.[15] Herein, we showed that DALDA enhanced AKT and GSK3β phosphorylation in the intestine *in vivo*, which correlated with protection from intestinal ischemia. The pharmacological agent, Ly294002, demonstrated that MOR-mediated protection from I/R injury requires activation of PI3K signaling. We confirmed these findings *in vitro*, showing that DALDA/MOR signaling directly activates the PI3K/Akt/GSK3β pathway. Furthermore, TUNEL and activated caspase-3 analysis showed that wortmannin reverses the DALDA-mediated protection against staurosporine-induced apoptosis.

The anti-apoptotic role of the PI3K signaling pathway has been observed in enterocytes,[34] and in endothelial cells subjected to hypoxic conditions.[35] Downstream, phospholipid-dependent Akt pathway activation has been implicated in the anti-apoptotic effects of PI3K activation.[19] Akt activation can lead to enhancement of prosurvival signaling through IκB kinase—mediated increases in NF-κB activity.[19] Akt activation can also directly inhibit apoptotic signals, such as Fas-L, Bax, and p53, and promotes anti-apoptotic signals, such as *Bcl-XL* and *Bcl-2*.[19] In addition, Akt activation results in GSK3β phosphorylation, leading to inhibition of apoptotic signals mediated by MCL-1 and Bax and enhancement of prosurvival signals, such as β-catenin.[19] Because DALDA failed to directly activate NF-κB signaling in IECs[14] and competitive inhibition of MOR abrogates GSK3β phosphorylation, the PI3K/Akt/GSK3β pathway is likely responsible for the anti-apoptotic effects of the opioid.

The functional impact of DALDA-mediated intestinal barrier enhancement through PI3K activity includes the prevention of microbial translocation. The presence of bacterial 16S rDNA in the liver of I/R-exposed mice was strongly decreased by DALDA administration. This is an important finding, because bacterial translocation across a damaged barrier is the main source of multiorgan failure in patients experiencing intestinal ischemia.[4,5,11]

Overall, these studies demonstrate, for the first time to our knowledge, that activation of IEC-specific, PI3K-dependent MOR signaling resulted in protection from ischemia/reperfusion-induced intestinal injury. The lack of therapies for treating intestinal ischemia, combined with the wide

availability of Food and Drug Administration–approved, MOR-specific agonists to clinicians, makes this work of particular clinical relevance.

Acknowledgments

J.R.G., E.P.-C., and P.N.Y. performed experiments; J.R.G., E.P.-C., P.N.Y., B.R., and C.J. designed experiments; J.W. contributed reagents; J.R.G., E.P.-C., and C.J. wrote the manuscript; and J.R.G., E.P.-C., J.W., and C.J. edited the manuscript.

References

1. Sartor RB: Microbial influences in inflammatory bowel diseases. Gastroenterology 2008, 134:577–594
2. Marchiando AM, Shen L, Graham WV, Edelblum KL, Duckworth CA, Guan Y, Montrose MH, Turner JR, Watson AJ: The epithelial barrier is maintained by in vivo tight junction expansion during pathologic intestinal epithelial shedding. Gastroenterology 2011, 140. 1208–1218. e1–2
3. Iizuka M, Konno S: Wound healing of intestinal epithelial cells. World J Gastroenterol 2011, 17:2161–2171
4. Haglund U: Gut ischaemia. Gut 1994, 35:S73–S76
5. Parks DA, Granger DN: Ischemia-reperfusion injury: a radical view. Hepatology 1988, 8:680–682
6. Young CM, Kingma SD, Neu J: Ischemia-reperfusion and neonatal intestinal injury. J Pediatr 2011, 158:e25–e28
7. Sturm A, Dignass AU: Epithelial restitution and wound healing in inflammatory bowel disease. World J Gastroenterol 2008, 14: 348–353
8. Guslandi M: Exacerbation of inflammatory bowel disease by nonsteroidal anti-inflammatory drugs and cyclooxygenase-2 inhibitors: fact or fiction? World J Gastroenterol 2006, 12:1509–1510
9. Maiden L, Thjodleifsson B, Theodors A, Gonzalez J, Bjarnason I: A quantitative analysis of NSAID-induced small bowel pathology by capsule enteroscopy. Gastroenterology 2005, 128:1172–1178
10. Kinross J, Warren O, Basson S, Holmes E, Silk D, Darzi A, Nicholson JK: Intestinal ischemia/reperfusion injury: defining the role of the gut microbiome. Biomark Med 2009, 3:175–192
11. Gustot T: Multiple organ failure in sepsis: prognosis and role of systemic inflammatory response. Curr Opin Crit Care 2011, 17:153–159
12. Koury J, Deitch EA, Homma H, Abungu B, Gangurde P, Condon MR, Lu Q, Xu DZ, Feinman R: Persistent HIF-1alpha activation in gut ischemia/reperfusion injury: potential role of bacteria and lipopolysaccharide. Shock 2004, 22:270–277
13. Chen LW, Egan L, Li ZW, Greten FR, Kagnoff MF, Karin M: The two faces of IKK and NF-kappaB inhibition: prevention of systemic inflammation but increased local injury following intestinal ischemia-reperfusion. Nat Med 2003, 9:575–581
14. Goldsmith JR, Uronis JM, Jobin C: Mu opioid signaling protects against acute murine intestinal injury in a manner involving Stat3 signaling. Am J Pathol 2011, 179:673–683
15. Gross ER, Hsu AK, Gross GJ: The JAK/STAT pathway is essential for opioid-induced cardioprotection: JAK2 as a mediator of STAT3, Akt, and GSK-3 beta. Am J Physiol Heart Circ Physiol 2006, 291:H827–H834
16. Li R, Wong GT, Wong TM, Zhang Y, Xia Z, Irwin MG: Intrathecal morphine preconditioning induces cardioprotection via activation of delta, kappa, and mu opioid receptors in rats. Anesth Analg 2009, 108:23–29
17. Wong GT, Huang Z, Ji S, Irwin MG: Remifentanil reduces the release of biochemical markers of myocardial damage after coronary artery bypass surgery: a randomized trial. J Cardiothorac Vasc Anesth 2010, 24:790–796
18. Law PY, Wong YH, Loh HH: Molecular mechanisms and regulation of opioid receptor signaling. Annu Rev Pharmacol Toxicol 2000, 40: 389–430
19. Duronio V: The life of a cell: apoptosis regulation by the PI3K/PKB pathway. Biochem J 2008, 415:333–344
20. Uronis JM, Muhlbauer M, Herfarth HH, Rubinas TC, Jones GS, Jobin C: Modulation of the intestinal microbiota alters colitis-associated colorectal cancer susceptibility. PLoS One 2009, 4:e6026
21. Joo Y, Karrasch T, Muhlbauer M, Allard B, Narula A, Herfarth H, Jobin C: Tomato lycopene extract prevents lipopolysaccharide-induced NF-κB signaling but worsens dextran sulfate sodium-induced colitis in NF-κB^{EGFP} mice. PLoS One 2009, 4:e4562
22. Schiller PW, Nguyen TM, Chung NN, Lemieux C: Dermorphin analogues carrying an increased positive net charge in their "message" domain display extremely high mu opioid receptor selectivity. J Med Chem 1989, 32:698–703
23. Jilling T, Lu J, Jackson M, Caplan MS: Intestinal epithelial apoptosis initiates gross bowel necrosis in an experimental rat model of neonatal necrotizing enterocolitis. Pediatr Res 2004, 55:622–629
24. Hoentjen F, Sartor RB, Ozaki M, Jobin C: STAT3 regulates NF-kappaB recruitment to the IL-12p40 promoter in dendritic cells. Blood 2005, 105:689–696
25. Roth BL, Laskowski MB, Coscia CJ: Evidence for distinct subcellular sites of opiate receptors: demonstration of opiate receptors in smooth microsomal fractions isolated from rat brain. J Biol Chem 1981, 256: 10017–10023
26. Trotter AJ, Parslow AC, Heath JK: Morphologic analysis of the zebrafish digestive system. Methods Mol Biol 2009, 546:289–315
27. Haller D, Russo MP, Sartor RB, Jobin C: IKKβ and phosphatidylinositol 3-kinase/Akt participate in non-pathogenic Gram-negative enteric bacteria-induced RelA phosphorylation and NF-κB activation in both primary and intestinal epithelial cell lines. J Biol Chem 2002, 277:38168–38178
28. Karrasch T, Spaeth T, Allard B, Jobin C: PI3K-dependent GSK3B(Ser9)-phosphorylation is implicated in the intestinal epithelial cell wound-healing response. PLoS One 2011, 6:e26340
29. Packey CD, Ciorba MA: Microbial influences on the small intestinal response to radiation injury. Curr Opin Gastroenterol 2009, 26: 88–94
30. Pickert G, Neufert C, Leppkes M, Zheng Y, Wittkopf N, Warntjen M, Lehr H-A, Hirth S, Weigmann B, Wirtz S, Ouyang W, Neurath MF, Becker C: STAT3 links IL-22 signaling in intestinal epithelial cells to mucosal wound healing. J Exp Med 2009, 206:1465–1472
31. Steinbrecher KA, Harmel-Laws E, Sitcheran R, Baldwin AS: Loss of epithelial RelA results in deregulated intestinal proliferative/apoptotic homeostasis and susceptibility to inflammation. J Immunol 2008, 180: 2588–2599
32. Feinman R, Deitch EA, Watkins AC, Abungu B, Colorado I, Kannan KB, Sheth SU, Caputo FJ, Lu Q, Ramanathan M, Attan S, Badami CD, Doucet D, Barlos D, Bosch-Marce M, Semenza GL, Xu DZ: HIF-1 mediates pathogenic inflammatory responses to intestinal ischemia-reperfusion injury. Am J Physiol Gastrointest Liver Physiol 2010, 299:G833–G843
33. Rollwagen FM, Madhavan S, Singh A, Li YY, Wolcott K, Maheshwari R: IL-6 protects enterocytes from hypoxia-induced apoptosis by induction of bcl-2 mRNA and reduction of fas mRNA. Biochem Biophys Res Commun 2006, 347:1094–1098
34. Leone V, di Palma A, Ricchi P, Acquaviva F, Giannouli M, Di Prisco AM, Iuliano F, Acquaviva AM: PGE2 inhibits apoptosis in human adenocarcinoma Caco-2 cell line through Ras-PI3K association and cAMP-dependent kinase A activation. Am J Physiol Gastrointest Liver Physiol 2007, 293:G673–G681
35. Hung S-C, Pochampally RR, Chen S-C, Hsu S-C, Prockop DJ: Angiogenic effects of human multipotent stromal cell conditioned medium activate the PI3K-Akt pathway in hypoxic endothelial cells to inhibit apoptosis, increase survival, and stimulate angiogenesis. Stem Cells 2007, 25:2363–2370